Journal of Colloid and Interface Science 368 (2012) 372–377

Contents lists available at SciVerse ScienceDirect

Journal of Colloid and Interface Science

www.elsevier.com/locate/jcis

Enhancement of DNA compaction by negatively charged nanoparticles: Effect of nanoparticle size and surfactant chain length

Sergii Rudiuk [a], Kenichi Yoshikawa [a], Damien Baigl [b,c,d,*]

[a] Department of Physics, Graduate School of Science, Kyoto University, Kyoto 606-8502, Japan
[b] Department of Chemistry, Ecole Normale Supérieure, 75005 Paris, France
[c] Université Pierre et Marie Curie Paris 6, 75005 Paris, France
[d] UMR 8640, CNRS, France

ARTICLE INFO

Article history:
Received 31 August 2011
Accepted 13 October 2011
Available online 20 October 2011

Keywords:
DNA
Nanoparticles
DNA compaction
Surfactant
Higher-order structure
Fluorescence microscopy

ABSTRACT

We study the compaction of genomic DNA by a series of alkyltrimethylammonium bromide surfactants having different hydrocarbon chain lengths n: dodecyl-(DTAB, $n = 12$), tetradecyl-(TTAB, $n = 14$) and hexadecyl-(CTAB, $n = 16$), in the absence and in the presence of negatively charged silica nanoparticles (NPs) with a diameter in the range 15–100 nm. We show that NPs greatly enhance the ability of all cationic surfactants to induce DNA compaction and that this enhancement increases with an increase in NP diameter. In the absence of NP, the ability of cationic surfactants to induce DNA compaction increases with an increase in n. Conversely, in the presence of NPs, the enhancement of DNA compaction increases with a decrease in n. Therefore, although CTAB is the most efficient surfactant to compact DNA, maximal enhancement by NPs is obtained for the largest NP diameter (here, 100 nm) and the smallest surfactant chain length (here, DTAB). We suggest a mechanism where the preaggregation of surfactants on NP surface mediated by electrostatic interactions promotes cooperative binding to DNA and thus enhances the ability of surfactants to compact DNA. We show that the amplitude of enhancement is correlated with the difference between the surfactant concentration corresponding to aggregation on DNA alone and that corresponding to the onset of adsorption on nanoparticles.

© 2011 Elsevier Inc. All rights reserved.

1. Introduction

Compaction is the process in which a DNA molecule undergoes a transition between an elongated conformation and a very compact form. In nature, DNA compaction occurs to package genomic material inside tiny spaces such as viral capsids and cell nuclei. In vitro, several strategies exist to compact DNA, offering promising applications in biotechnologies and materials science [1]. As a negatively charged polyelectrolyte, DNA can be compacted by a variety of cationic agents [2] such as polyamines [2,3], polymers [4–7], nanoparticles [8,9], vesicles [10] and surfactants [11–21]. Among the large variety of compaction agents, cationic surfactants have attracted a particular attention due to the applications in isolation and purification of DNA as well as in gene delivery [22–24]. Moreover, using a cationic surfactant containing an azobenzene photosensitive moiety, the control by light of DNA higher-order structure has been achieved [15,25,26], and this effect has been successfully applied to control by light gene expression systems at both transcription and translation levels [27]. However, a major drawback of surfactants for biology-related studies relies in their cytotoxicity [28]. Finding way to decrease this cytotoxicity is thus a crucial challenge. A typical approach consists in the modification of surfactant's headgroup [29,30] or chain length [31]. Another way to decrease the cytotoxicity of a given surfactant is to improve its DNA compaction efficiency, that is, to decrease the surfactant concentration necessary for DNA compaction. Recently it was shown that very small amounts of anionic silica nanoparticles (10^{-4}–10^{-2} wt%) significantly decreased the concentration of surfactant needed to induce DNA compaction [32]. This was demonstrated on NPs with a diameter 100 nm and a standard (DTAB) or a photosensitive (AzoTAB) surfactant having similar hydrophobicity and chain length. To better understand this counter-intuitive phenomenon, we performed for the first time a systematic study of the effects of NP diameter and surfactant chain length. This allowed us to determine optimal conditions for nanoparticle-induced enhancement of DNA compaction by cationic surfactants as well as to propose a cooperative mechanism of interaction between surfactants, NPs and DNA.

* Corresponding author at: Department of Chemistry, Ecole Normale Supérieure, 24 rue Lhomond, 75005 Paris, France. Fax: +33 1 4432 2402.
E-mail address: damien.baigl@ens.fr (D. Baigl).
URL: http://www.baigllab.com/ (D. Baigl).

0021-9797/$ - see front matter © 2011 Elsevier Inc. All rights reserved.
doi:10.1016/j.jcis.2011.10.033

2. Materials and methods

2.1. Materials

Bacteriophage T4 DNA (166 kbp) was from Wako Chemicals, YOYO-1 iodide was from Molecular Probes. Surfactants: DTAB, TTAB and CTAB were from TCI (Tokyo, Japan). Naked silica nanoparticles (30 wt% in isopropanol) of 15, 40 and 100 nm diameter (NP15, NP40 and NP100) were a gift from Nissan Chemicals. They were diluted in water to prepare stock solutions of 10^{-2} wt%, 10^{-1} wt% and 10^{-1} wt% in water for NP15, NP40 and NP100, respectively. All other chemicals were from Sigma. Deionised water (Millipore, 18 MΩ cm) was used for all experiments.

2.2. Preparation of DNA samples

Water, Tris–HCl buffer, surfactant (DTAB, TTAB or CTAB), silica nanoparticles (NP100, NP40 or NP15), and YOYO-1 iodide were mixed in this order prior to careful T4 DNA introduction under low shear conditions to avoid DNA breakage [33]. In order to permit the efficient adsorption of the surfactant on nanoparticles, the samples were equilibrated for 15 min after vigorous mixing of surfactant with NPs. After addition of YOYO and DNA, the samples were equilibrated for a second time for 15 min prior to observation of the nucleic acid by fluorescence microscopy. Equilibration steps before and after DNA introduction were systematically applied to get reproducible data. For all experiments, we used T4 DNA at a final concentration of 0.1 μM (concentration in nucleotides) in Tris–HCl buffer (10 mM, pH 7.4) with YOYO (0.01 μM) as a DNA fluorescent dye. All experiments were performed at room temperature.

2.3. Fluorescence microscopy (FM)

Fluorescence microscopy was performed using an Axiovert 135 TV (Zeiss) microscope equipped with a 100× oil-immersion lens. Images were recorded using an EB-CCD camera and an image processor Argus 10 (Hamamatsu Photonics). DNA molecules stained with YOYO were observed in 20 μL microdroplets deposited on a clean glass cover slide. Under these conditions the compaction states of DNA are clearly distinguishable: DNA molecules in the compact state appear as bright fast-diffusing spots, whereas DNA molecules in the coil state have a much larger apparent long-axis length, a much lower translational diffusion coefficient and exhibits characteristic intrachain thermal fluctuations. For each observation, a minimum of 150 individual DNA molecules were characterized to determine the fraction of molecules in the compact state.

2.4. Zeta potential measurements

Zeta potential of 100 nm silica nanoparticles (NP100) was measured with Zetasizer Nano-ZS (Malvern Instruments) at 25 °C. Mixtures of NP100 (of final concentration 1.5×10^{-3} wt%) and increasing amounts of surfactants (DTAB, TTAB or CTAB) were prepared in 10 mM Tris–HCl buffer (pH 7.4). After mixing, the samples were equilibrated for 15 min at room temperature prior to zeta potential measurements. Each measurement was repeated 10 times. The changes in mean zeta potential were then plotted against surfactant concentration.

3. Results

3.1. Experimental system

We studied the compaction of T4 DNA (166 kbp) by 3 alkyltrimethylammonium bromide surfactants having different hydrocarbon chain lengths n, dodecyl-(DTAB, $n = 12$), tetradecyl-(TTAB, $n = 14$) and hexadecyl-(CTAB, $n = 16$) (Fig. 1A), in the presence and in the absence of silica nanoparticles of different diameters d: NP15 ($d \approx 15$ nm), NP40 ($d \approx 40$ nm), and NP100 ($d \approx 100$ nm) (Fig. 1B). These nanoparticles have a narrow size polydisersity [8,9] and their mean diameter is displayed in Fig. 1B. A typical experiment consisted in mixing surfactant and nanoparticles prior to addition of DNA and fluorescent probe (YOYO-1 iodide) (Fig. 1C). Fluorescence microscopy was used to characterize the conformation of a large amount of individual DNA molecules (>150 per observation). With this technique, we could discriminate between DNA molecules in the compact state,

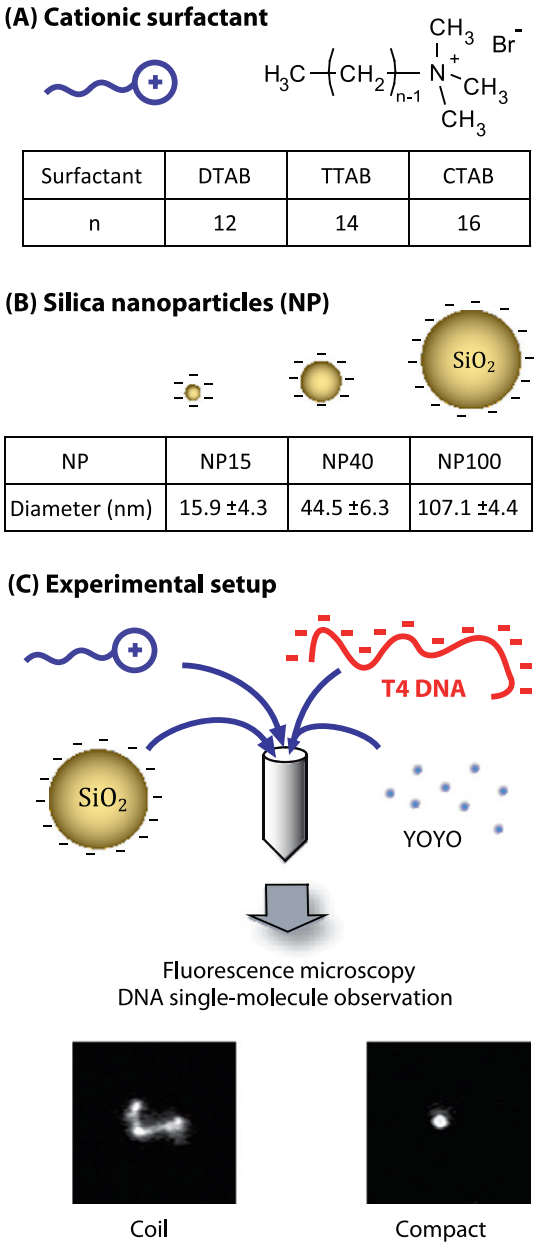

Fig. 1. Experimental system. (A) Cationic trimethylammonium surfactants having $n = 12$, 14 and 16 carbon atoms in the hydrophobic tail were used to induce the compaction of T4 DNA. (B) Silica nanoparticles with various diameters were used to enhance the compaction of DNA by surfactants. The table shows the mean diameter as measured by dynamic light scattering. (C) Top: a typical experiments consisted in mixing surfactants with nanoparticles prior to addition of T4 DNA and YOYO-1 fluorescent dye and single-molecule observation by fluorescence microscopy. Bottom: typical images of a single DNA molecule in the coil state (left) and in the compact state (right). Each image has a size 5 μm × 5 μm.

which appeared as bright fast-diffusing spots (Fig. 1C, right picture), and DNA molecules in the coil state, which have a much larger apparent long-axis length, a slower diffusion coefficient and typical intrachain fluctuations (Fig. 1C, left picture). For each solution composition, this allowed us to establish a compaction curve where the fraction of individual DNA molecules in the compact state was plotted as a function of surfactant concentration.

3.2. Enhancement of DNA compaction by silica nanoparticles

Fig. 2 shows compaction curves by DTAB in the absence and in the presence of a fixed concentration of NP100 (1.5×10^{-3} wt%). Without NP, for $0 \leqslant [DTAB] \leqslant 400$ μM, most of DNA molecules are in the coil state. For $400 \leqslant [DTAB] \leqslant 1000$ μM, the fraction of DNA molecules in the compact state strongly increases to reach 100% at about [DTAB] = 1000 μM. For $[DTAB] \geqslant 1000$ μM, all DNA molecules are in the compact state. This compaction curve has a sigmoidal shape, which is typically observed in DNA-surfactant systems and characteristic of a cooperative process [14,15,34].

In the presence of NP100, the compaction curve has a very similar shape but it is shifted toward lower DTAB concentrations. For instance, for [DTAB] = 300 μM, 0.5% and 97% of DNA molecules are in the compact state, in the absence and in the presence of NP100, respectively. From these compaction curves, we can also estimate $[DTAB]^*_{50}$ and $[DTAB]_{50}$, which are the concentrations of DTAB needed to reach 50% of compaction in the absence and in the presence of nanoparticles, respectively. For [NP100] = 1.5×10^{-3} wt%, we found $[DTAB]^*_{50}$ = 715 μM and $[DTAB]_{50}$ = 120 μM. All these results confirm that the presence of a small amount of silica nanoparticles with a diameter d = 100 nm greatly enhances the efficiency of DTAB cationic surfactant to compact DNA. As a possible mechanism, we suggest that negatively charged nanoparticles induce the aggregation of surfactant molecules through electrostatic interactions, promote cooperative binding to DNA and thus enhance the ability of surfactants to compact DNA [32]. Note that for the whole concentration range of NPs used in this study, that is from 10^{-5} wt% to 10^{-2} wt%, NPs alone did not induce DNA compaction, regardless of NP size. This shows that DNA compaction is not induced by a crowding effect such as that observed in the presence of negatively charged proteins [35,36]. Compaction is thus here mainly induced by cationic surfactants, and their efficiency to compact DNA is enhanced in the presence of negatively charged NPs.

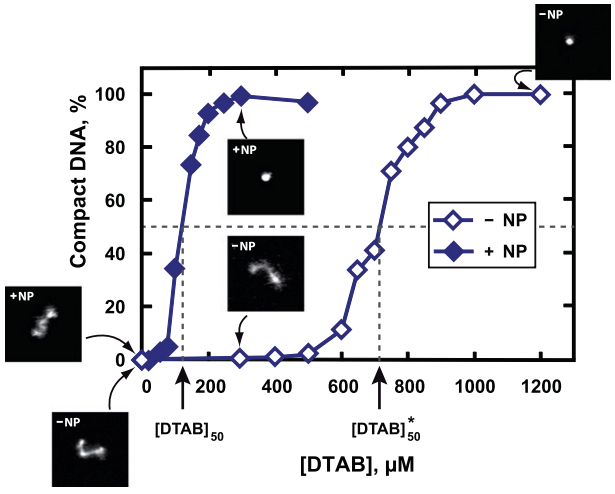

Fig. 2. Enhancement of DTAB-induced DNA compaction by 100 nm silica nanoparticles (NP100). Compaction curves (fraction of DNA molecules in the compact state as a function of DTAB concentration) and typical fluorescence microscopy images of DNA molecules in solution in the absence (−NP) and in the presence (+NP) of 100 nm silica nanoparticles. Horizontal dashed line corresponds to 50% of DNA molecules in the compact state. Vertical dashed lines show the concentrations of DTAB corresponding to 50% of DNA molecules in the compact state, in the absence and presence of NP100 ($[DTAB]^*_{50}$ and $[DTAB]_{50}$, respectively). Each image has a size 5 μm × 5 μm. [DNA] = 0.1 μM; [YOYO] = 0.01 μM; [NP100] = 1.5×10^{-3} wt%; [Tris–HCl] = 10 mM (pH = 7.4).

3.3. Effect of nanoparticle size and concentration

We studied the effect of nanoparticle size and concentration on the efficiency of this enhancement. For each condition, we established the compaction curve of DNA by DTAB in the presence and in the absence of NPs and we measured $[DTAB]^*_{50}$ and $[DTAB]_{50}$ as described in Fig. 2. Fig. 3A shows the ratio $R = [DTAB]_{50}/[DTAB]^*_{50}$ as a function of NP concentration for NP15, NP40 and NP100. It shows that the presence of NPs decreases the DTAB concentration corresponding to DNA compaction ($R < 1$) regardless of NP diameter. Moreover, we observe an optimal NPs concentration, for which the enhancement of DNA compaction is maximal (R is minimal). This optimal concentration exists for all NPs but it significantly increases with an increase in NP diameter (1.1×10^{-4} wt%, 3×10^{-4} wt% and 1.5×10^{-3} wt% for NP15, NP40 and NP100, respectively).

The amplitude of the enhancement at the optimal concentration also depends on NP size and is observed to increase with an increase in NP size. At optimal concentrations, NP15, NP40 and NP100 decrease the concentration of DTAB corresponding to 50% of DNA compaction 1.6-fold (from 715 to 445 μM), 4.0-fold (from 715 to 180 μM) and 6.0-fold (from 715 to 120 μM), respectively. The existence of an optimal NPs concentration can be explained

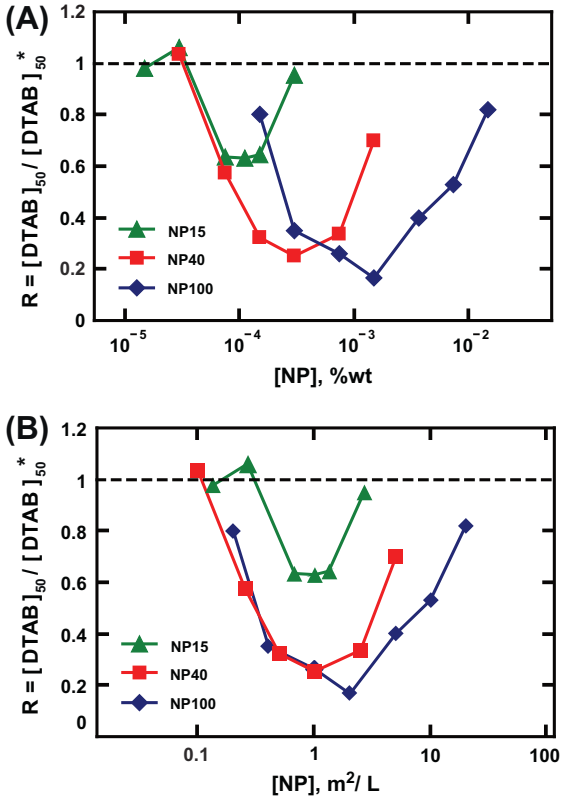

Fig. 3. Effect of NP size and concentration on the enhancement of DNA compaction by DTAB. Ratio R of surfactant concentrations corresponding to 50% of DNA compaction in the presence ($[DTAB]_{50}$) and in the absence ($[DTAB]^*_{50}$) of NPs as a function of: (A) NP weight concentration and (B) NP surface concentration. Symbols are data points. Lines connecting symbols are guides for the eyes. [DNA] = 0.1 μM; [YOYO] = 0.01 μM; [Tris–HCl] = 10 mM (pH = 7.4).

as follows. At low NPs concentrations, the concentration of nucleation sites is small and the cooperative effects are limited. With an increase in NPs concentration, the concentration of nucleation sites increases and the enhancement in DNA compaction becomes larger. This holds true as long as the number of aggregated surfactants per nanoparticle is maximal. When NPs concentration becomes too large, surfactants can still interact with NPs but the number of aggregated surfactants per nanoparticle decreases and effects of cooperativity weaken. With a further increase in NPs concentration, this 'dilution' effect increases thus decreasing the ability of surfactants to induce compaction. This mechanism suggests that the optimal aggregation of DTAB on nanoparticles occurs at the same surface concentration of silica in the solution. To test this hypothesis, we plotted the ratio R as a function of the silica surface concentration for the different nanoparticle sizes (Fig. 3B). This analysis shows that the optimal enhancement for different NPs correspond to very close surface concentration, regardless of NP size (1.02 m^2/L for NP15 and NP40, and 2.05 m^2/L for NP100). This confirms that the primary role of nanoparticles in the enhancement of DNA compaction is to act as nucleation centers for the aggregation of surfactants mediated through electrostatic interactions between nanoparticle negatively charged surfaces and surfactant cationic heads. The decrease in the efficiency to enhance DNA compaction with a decrease in NP size can be attributed to the rigidity of DNA, which has a persistence length l_p of the order of 50 nm. For instance, it has been shown that the compaction efficiency of cationic NPs strongly decreases with a decrease in NP size for NPs having a diameter smaller than l_p [8,9].

3.4. Effect of surfactant chain length

First, DNA compaction curves were established in the absence of NPs for DTAB, TTAB and CTAB having n = 12, 14 and 16 carbon atoms in their hydrophobic tail, respectively (Fig. 4).

It shows that DNA compaction is significantly shifted to smaller surfactant concentrations with an increase in n. For instance, let $[surf]^*_{50}$ be the surfactant concentration necessary to induce 50% of DNA compaction in the absence of NP. We found $[surf]^*_{50}$ = 715 μM, 28.5 μM and 6.5 μM for n = 12, 14 and 16, respectively. This is in agreement with previous observations on similar systems [14–16] and can be explained by the cooperative nature of surfactant/DNA interaction. With an increase in n, that is, hydrophobicity of the tail, cationic surfactants are more prone to aggregation, which is confirmed by the decrease in their CMC (15 mM, 3.2 mM and 0.85 mM at 25 °C for n = 12, 14 and 16, respectively [37]). This enhances the efficiency of surfactants to cooperatively bind to DNA through electrostatic interactions and therefore promotes DNA compaction at a lower surfactant concentration.

Then, we established these compaction curves in the presence of different concentrations and sizes of NPs. Fig. 5 shows the ratio $R = [surf]_{50}/[surf]^*_{50}$ ($[surf]_{50}$ is the surfactant concentration to achieve 50% of DNA compaction in the presence of NPs) as a function of NP concentration for different NP sizes and surfactant chain length. First, it shows that, for a given NP size, the enhancement is maximal for intermediate NP concentration and that the corresponding optimal NP concentration does not vary with a change in surfactant chain length. This effect is observed for all NP sizes. It confirms that nanoparticles act as nucleation centers for the aggregation of cationic surfactants through electrostatic interac-

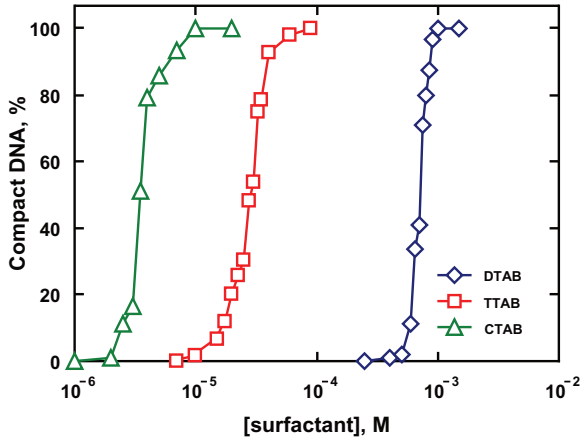

Fig. 4. DNA compaction by DTAB, TTAB and CTAB in absence of NP. Symbols are data points. Lines connecting symbols are guides for the eyes. [DNA] = 0.1 μM; [YOYO] = 0.01 μM; [Tris–HCl] = 10 mM (pH = 7.4).

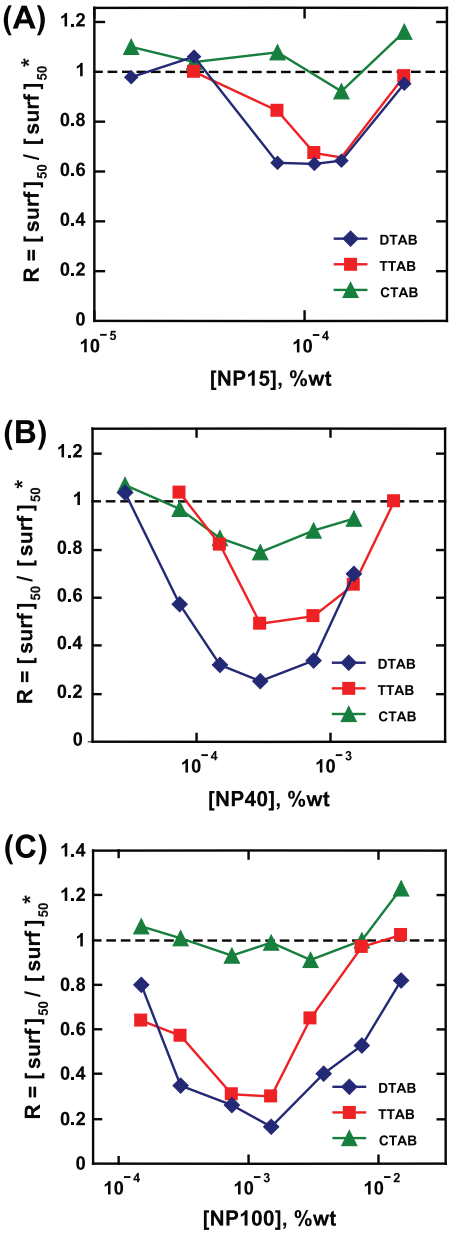

Fig. 5. Effect of surfactant chain length on enhancement of DNA compaction in the presence of NPs. Ratio R of surfactant concentrations corresponding to 50% of DNA compaction in the presence ($[surf]_{50}$) and in the absence ($[surf]^*_{50}$) of NPs as a function of concentration of: (A) NP15, (B) NP40 and (C) NP100. Symbols are data points. Lines connecting symbols are guides for the eyes. [DNA] = 0.1 μM; [YOYO] = 0.01 μM; [Tris–HCl] = 10 mM (pH = 7.4).

tions and are therefore not sensitive to the hydrophobicity of surfactant chain length.

Interestingly, while Fig. 4 shows that compaction efficiency of surfactant without NPs increases with surfactant chain length, Fig. 5 shows that the amplitude of enhancement in the presence of NPs follows the opposite trend and strongly decreases with n, regardless of NP diameter. At optimal NP100 concentration (1.5×10^{-3} wt%), the presence of NPs induces a decrease of surfactant concentration necessary to induce 50% of DNA compaction by a factor of 6.0 (from 715 to 120 μM), 3.3 (from 28.5 to 8.7 μM) and 1.1 (from 6.5 to 5.9 μM) for n = 12, 14 and 16, respectively. Similar results were observed for NP40. At optimal NP40 concentration (3×10^{-4} wt%), surfactant concentration is decreased by a factor of 4.0 (from 715 to 180 μM), 2.0 (from 28.5 to 14.0 μM) and 1.25 (from 6.5 to 5.2 μM) for n = 12, 14 and 16, respectively. The enhancement efficiency of NP15 is much lower (Fig. 5A) and, at optimal NP15 concentration (1.1×10^{-4} wt%), surfactant concentration is decreased by a factor of 1.6 (from 715 to 450 μM), 1.5 (from 28.5 to 19.0 μM) and 1.1 (from 6.5 to 6.0 μM) for n = 12, 14 and 16, respectively.

4. Discussion

All our results suggest that the enhancement of DNA compaction in the presence of NPs is due to the aggregation of surfactants on NP surface through electrostatic interactions. To further explore this mechanism, we followed the electrostatic interaction between surfactants and NP100 by zeta (ζ) potential measurements. Fig. 6A shows ζ potential of NP100 as a function of surfactant concentration for a concentration of NP100 corresponding to the maximal enhancement (1.5×10^{-3} wt%) and different surfactant chain lengths n.

Regardless on n, the curves have a similar general trend with two characteristic parts depending on surfactant concentration. At a low concentration, ζ is almost constant or slightly increases but remains close to the value for bare silica NPs (−27 ± 3 mV). In this regime, cationic surfactants have thus no or few interactions with NPs. In contrast, for sufficiently high concentrations, ζ strongly increases with an increase in surfactant concentration up to positive values. This observation indicates that cationic surfactants electrostatically adsorb on the negatively charged surface of NPs, forming a first monolayer onto which additional surfactant molecules can adsorb by hydrophobic interactions. Similar phenomenon has been reported with the cationic surfactant cetyltrimethylammonium bromide (CTAB), which was shown to form bilayers or multilayers on silica NPs and induced a change of ζ from about −30 mV to +(20–50) mV [38,39]. Phenomenologically, we can thus use the concentration at the transition between these two regimes as an estimation of the onset of the adsorption of surfactants on NPs surface. This concentration is noted $[surf]_{adsorption}$ and is represented as vertical dashed lines in Fig. 6A. Fig. 6A shows that $[surf]_{adsorption}$ decreases with an increase in surfactant chain length ($[surf]_{adsorption}$ = 170 μM, 9.0 μM and 2.0 μM for n = 12, 14 and 16, respectively), which is in agreement with previous reports on the adsorption of cationic surfactants on silica and ZnS NPs [40,41]. This can be explained by the increase in the propensity of surfactants to form aggregates when the hydrophobicity of the chain increases. Fig. 6B shows DNA compaction by DTAB, TTAB and CTAB, in the presence (filled symbols) and absence (open symbols) of NP100 at optimal concentration (1.5×10^{-3} wt%). Interestingly, DNA compaction in the presence of NPs occurs for surfactant concentration around the onset of surfactant adsorption on NPs, as estimated from ζ potential measurements (dashed lines in Fig. 6A and B). This observation confirms that pre-aggregation of surfactants on NPs is responsible of the enhanced DNA compaction by surfactants in the presence of NPs. The enhancement efficiency can thus be analyzed in terms of the difference between concentrations of surfactant corresponding to aggregation on

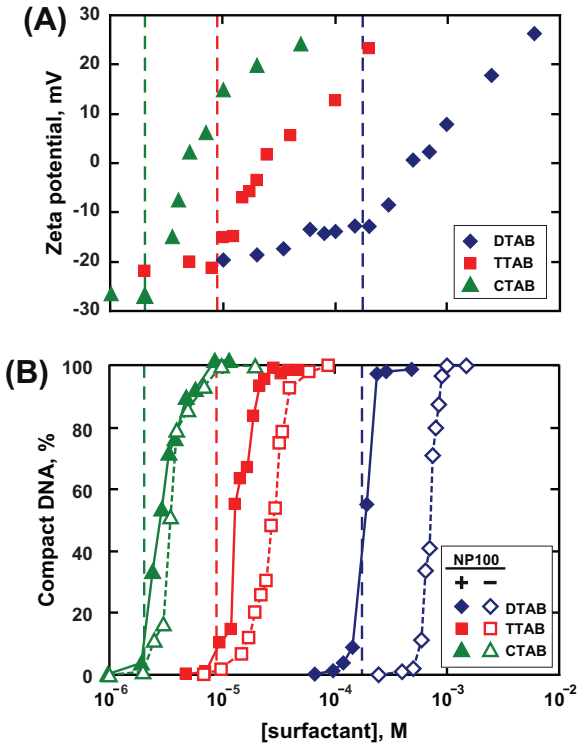

Fig. 6. Comparison of DTAB, TTAB and CTAB concentrations corresponding to (A) adsorption on NP100 and (B) DNA compaction in the presence of NP100. (A) Zeta potential as function of surfactant concentration in the absence of DNA. (B) DNA compaction curves in presence (filled symbols) and absence (open symbols) of NP100. Symbols are data points. Lines connecting symbols are guides for the eyes. [DNA] = 0.1 μM; [NP100] = 1.5×10^{-3} wt%; [Tris–HCl] = 10 mM (pH = 7.4).

DNA alone (which can be estimated by $[surf]^*_{50}$) and that corresponding to adsorption on nanoparticles alone ($[surf]_{adsorption}$). Enhancement of DNA compaction is observed when $[surf]_{adsorption} < [surf]^*_{50}$, that is, when surfactants aggregate on NPs surface at a concentration lower than that on DNA alone. Moreover, the amplitude of enhancement of DNA compaction increases with an increase in the difference between $[surf]^*_{50}$ and $[surf]_{adsorption}$. For instance, for NP100 at optimal concentration, the enhancement $1/R$ equals 6.0, 3.3 and 1.1 while the difference ($[surf]^*_{50} - [surf]_{adsorption}$) equals 545 μM, 19.5 μM and 4.5 μM for n = 12, 14 and 16, respectively. This effect can be explained by the following mechanism. In the absence of NP, surfactants with a higher hydrophobicity induce DNA compaction at a lower concentration (Fig. 4) because they are more prone to spontaneously form aggregates and therefore to cooperatively bind to DNA. Conversely, the presence of nanoparticles induces aggregation of surfactants on NP surface through electrostatic interactions, thus enhancing the natural ability of surfactants to induce DNA compaction. This effect will be all the more pronounced that surfactants have a low tendency to spontaneously aggregate in the absence of NP, that is, when they have a lower hydrophobicity. This explains the increase in enhancement with a decrease in hydrophobicity regardless of NP size (Fig. 5).

5. Conclusions

Very recently, negatively charged nanoparticles (NPs) were shown to enhance the ability of cationic surfactants to induce DNA compaction [32]. Here, we studied for the first time the influence of nanoparticle size and surfactant chain length on this phenomenon. Regardless of NPs' size, the enhancement is maximal for an intermediate concentration of NPs, which corresponds to optimal aggregation of surfactant molecules on the nanoparticles. It was

shown that the increase in NPs' size from 15 to 100 nm leads to an increase in the enhancement efficiency. Optimal enhancement was obtained for a similar surface concentration but, due to DNA rigidity, larger NPs are more efficient to promote DNA compaction. In the absence of NP, the ability of cationic surfactants to induce DNA compaction increased with an increase in surfactant hydrophobicity. We proposed a mechanism where the pre-aggregation of surfactants on NPs' surface mediated by electrostatic interactions promoted cooperative binding to DNA and thus enhanced the ability of surfactants to compact DNA. The enhancement amplitude of DNA compaction could thus be associated with the difference between surfactant concentration corresponding to aggregation on DNA alone ($[\text{surf}]^*_{50}$) and that corresponding to adsorption on nanoparticles alone ($[\text{surf}]_{\text{adsorption}}$). Enhancement was observed to increase with an increase in ($[\text{surf}]^*_{50} - [\text{surf}]_{\text{adsorption}}$), that is, with a decrease in surfactant hydrophobicity. This study thus constitutes a physico-chemical background for the further development of DNA-NP-surfactant systems, with possible applications in fields as diverse as transfection, in vitro gene expression and DNA-based nanomachines.

Acknowledgments

The research leading to these results has received funding from the Japan Science and Technology Agency under the ICORP 2006 "Spatio-Temporal Order" Project, the Institut Universitaire de France, and the European Research Council under the European Community's Seventh Framework Programme (FP7/2007-2013)/ ERC Grant agreement no. 258782.

References

[1] A. Estévez-Torres, D. Baigl, Soft Matter 7 (2011) 6746.
[2] L.C. Gosule, J.A. Schellman, Nature 259 (1976) 333.
[3] D. Baigl, K. Yoshikawa, Biophys. J. 88 (2005) 3486.
[4] U.K. Laemmli, Proc. Natl. Acad. Sci. USA 72 (1975) 4288.
[5] R.S. Dias, A. Pais, M.G. Miguel, B. Lindman, J. Chem. Phys. 119 (2003) 8150.
[6] T. Akitaya, A. Seno, T. Nakai, N. Hazemoto, S. Murata, K. Yoshikawa, Biomacromolecules 8 (2007) 273.
[7] W.-H. Huang, A.A. Zinchenko, C. Pawlak, Y. Chen, D. Baigl, ChemBioChem 8 (2007) 1771.
[8] A.A. Zinchenko, K. Yoshikawa, D. Baigl, Phys. Rev. Lett. 95 (2005) 228101.
[9] A.A. Zinchenko, T. Sakaue, S. Araki, K. Yoshikawa, D. Baigl, J. Phys. Chem. 111 (2007) 3019.
[10] A. Diguet, D. Baigl, Langmuir 24 (2008) 10604.
[11] S.M. Mel'nikov, V.G. Sergeyev, K. Yoshikawa, J. Am. Chem. Soc. 117 (1995) 2401.
[12] D. Matulis, I. Rouzina, V.A. Bloomfield, J. Am. Chem. Soc. 124 (2002) 7331.
[13] C.H. Spink, J.B. Chaires, J. Am. Chem. Soc. 119 (1997) 10920.
[14] R. Dias, S. Mel'nikov, B. Lindman, M.G. Miguel, Langmuir 16 (2000) 9577.
[15] A. Diguet, N.K. Mani, M. Geoffroy, M. Sollogoub, D. Baigl, Chem. Eur. J. 16 (2010) 11890.
[16] S. Rudiuk, S. Franceschi-Messant, N. Chouini-Lalanne, E. Perez, I. Rico-Lattes, Langmuir 24 (2008) 8452.
[17] M. Geoffroy, D. Faure, R. Oda, D.M. Bassani, D. Baigl, ChemBioChem 9 (2008) 2382.
[18] A. González-Pérez, J. Carlstedt, R.S. Dias, B. Lindman, Colloids Surf., B 76 (2010) 20.
[19] S. Bhattacharya, S.S. Mandal, Biochemistry 37 (1998) 7764.
[20] R.S. Dias, B. Lindman, M.G. Miguel, J. Phys. Chem. B 106 (2002) 12608.
[21] R.S. Dias, J. Innerlohinger, O. Glatter, M.G. Miguel, B. Lindman, J. Phys. Chem. B 109 (2005) 10458.
[22] D.D. Lasic, Liposome in Gene Delivery, CRC Press, Boca Raton, FL, 1997.
[23] L. Huang, M.C. Hung, E. Wagner, Non-Viral Vectors for Gene Therapy, Academic Press, New York, 1999.
[24] P.L. Felgner, G.M. Ringold, Nature 337 (1989) 387.
[25] A.-L.M. Le Ny, C.T. Lee Jr., J. Am. Chem. Soc. 128 (2006) 6400.
[26] M. Sollogoub, S. Guieu, M. Geoffroy, A. Yamada, A. Estévez-Torres, K. Yoshikawa, D. Baigl, ChemBioChem 9 (2008) 1201.
[27] A. Estévez-Torres, C. Crozatier, A. Diguet, T. Hara, H. Saito, K. Yoshikawa, D. Baigl, Proc. Natl. Acad. Sci. USA 106 (2009) 12219.
[28] J. You, M. Kamihira, S. Iijima, Cytotechnology 25 (1997) 45.
[29] A. Dasgupta, A.P. Das, R.S. Dias, M.G. Miguel, B. Lindman, V.M. Jadhav, M. Gnanamani, S. Maiti, J. Phys. Chem. B 111 (2007) 8502.
[30] V. Jadhav, S. Maiti, A. Dasgupta, P.K. Das, R. Dias, M.G. Miguel, B. Lindman, Biomacromolecules 9 (2008) 1852.
[31] H.M. Courrier, M.P. Krafft, N. Butz, C. Porte, N. Frossard, A. Remy-Kristensen, Y. Mely, F. Pons, T.F. Vandamme, Biomaterials 24 (2003) 689.
[32] S. Rudiuk, K. Yoshikawa, D. Baigl, Soft Matter 7 (2011) 5854.
[33] L. Cinque, Y. Ghomchi, Y. Chen, A. Bensimon, D. Baigl, ChemBioChem 11 (2010) 340.
[34] K. Hayakawa, J.P. Santerre, J.C.T. Kwak, Biophys. Chem. 17 (1983) 175.
[35] M.K. Krotova, V.V. Vasilevskaya, N. Makita, K. Yoshikawa, A.R. Khokhlov, Phys. Rev. Lett. 105 (2010) 128302.
[36] K. Yoshikawa, S. Hirota, N. Makita, Y. Yoshikawa, J. Phys. Chem. Lett. 1 (2010) 1763.
[37] M.J. Rosen, Surfactants and Interfacial Phenomena, third ed., John Wiley & Sons, Inc., Hoboken, NJ, 2004.
[38] E.Yu. Bryleva, N.A. Vodolazkaya, N.O. McHedlov-Petrossyan, L.V. Samokhina, N.A. Matveevskaya, A.V. Tolmachev, J. Colloid Interface Sci. 316 (2007) 712.
[39] B.P. Binks, J.A. Rodrigues, W.J. Frith, Langmuir 23 (2007) 3626.
[40] Z.-G. Cui, L.-L. Yang, Y.-Z. Cui, B.P. Binks, Langmuir 26 (2010) 4717.
[41] S.K. Mehta, S. Kumar, M. Gradzielski, J. Colloid Interface Sci. 360 (2011) 497.